Received: 25 September 2018 | Revised: 30 November 2018 | Accepted: 20 December 2018

DOI: 10.1002/aoc.4805

SPECIAL ISSUE ARTICLE

WILEY Applied Organometallic Chemistry

Synthesis and characterization of MgO nanoparticles supported on ionic liquid-based periodic mesoporous organosilica (MgO@PMO-IL) as a highly efficient and reusable nanocatalyst for the synthesis of novel spirooxindole-furan derivatives

Robabeh Baharfar[1] | Daryoush Zareyee[2] | Seyedeh Leila Allahgholipour[1]

[1]Department of Organic Chemistry, Faculty of Chemistry, University of Mazandaran, 4741695447 Babolsar, Iran

[2]Department of Chemistry, Qaemshahr Branch, Islamic Azad University, Qaemshar, Iran

Correspondence
Robabeh Baharfar, Department of Organic Chemistry, Faculty of Chemistry, University of Mazandaran, 4741695447, Babolsar, Iran.
Email: baharfar@umz.ac.ir

The synthesis and catalytic application of a novel MgO containing periodic mesoporous organosilica with ionic liquid framework (MgO@PMO-IL) is described. The prepared MgO@PMO-IL was characterized by Fourier transform-infrared spectroscopy, N_2 adsorption/desorption, transmission electron microscopy, field emission-scanning electron microscopy, thermogravimetric and inductively coupled plasma analyses. This nanocatalyst was successfully applied as a highly efficient and recoverable catalyst for the synthesis of novel spirooxindole-furan derivatives via the three-component reaction of 1,3-dicarbonyl compounds, *N*-phenacyl pyridinium salts and isatin derivatives. The products were achieved in high to excellent yields with a simple work-up procedure and short reaction times, and the catalyst could be recovered through a simple filtration process and successfully reused seven times without any significant decrease in its efficiency.

KEYWORDS
multi-component reaction, nanocatalyst, nanoparticles, novel spirooxindole-furan derivatives, periodic mesoporous organosilica

1 | INTRODUCTION

Spirocyclic compounds with a nitrogen-containing ring system fused at a central carbon, particularly spirooxindoles, are important heterocyclic compounds playing fundamental roles in pharmacological and biological fields.[1] Spirooxindole derivatives have been used as antitumor,[2] antimicrobial,[3] antibiotic, anti-HIV,[4] antimalarial,[5] anti-Alzheimer and anti-tuberculosis agents.[1] On the other hand, heterocyclic compounds containing furan rings have effective pharmacological activities, such as antidepressant, antimicrobial, antifungal and anti-inflammatory properties.[6]

Synthesis of spirooxindole-furan derivatives has been performed through the interrupted Feist–Benary reaction (IFB)[7] under homogeneous conditions in the presence of organic and inorganic base catalysts, such as K_2CO_3, DBU, DABCO, DIPEA and NEt_3.[8] However, these methods suffer from some disadvantages, including toxicity and expensiveness, difficult work-up and catalyst recovery processes,[8–14] long reaction times,[8,11–14] low reaction yields,[9,10,12] high amounts of catalyst,[9,11–13] and non-ecofriendly reaction conditions.[8–14] To overcome these problems, recently some recoverable heterogeneous catalysts have been developed.[15–19]

In the past few years, periodic mesoporous organosilica (PMO) hybrid nanomaterials have attracted much attention because of their uniform pore sizes, large pore volumes, high surface areas, high loading of organic functional groups, and good thermal and mechanical stability.[20,22–31]

Ionic liquids (ILs) are liquid salts with low-temperature melting points (< 100°C), which are used as media for different applications in various chemical processes. These materials are good solvents for catalytic reactions and have many advantages, such as easy separation, very low vapor pressure, non-flammability, high thermal stability and low toxicity.[32–36]

Ionic liquid-based PMO (PMO-IL) is an efficient support for metal catalysts, and can be recovered and reused several times without any remarkable decrease in its activity and efficiency.[22–25]

Metal oxide nanoparticles such as magnesium oxide (MgO-NPs) have been used as heterogeneous catalysts in the synthesis of numerous organic compounds because of their high surface area leading to small particle site and high concentration of corner/edge. In addition, MgO nanoparticles have a dual role that contains a number of (O^{2-}/O^{-}) as anionic oxidic Lewis basic and OH as a hydroxylic Brønsted basic site along with Mg^{2+} as a Lewis acid site.[37] For these reasons, we immobilized MgO nanoparticles on PMO-IL for the first time for the synthesis of a novel nanocatalyst as MgO@PMO-IL.

Due to expanding the scope of the IFB reaction, and in continuation of our previous works for the synthesis of novel heterocyclic compounds using heterogeneous catalysts,[37–40] we have developed a strategy for the preparation of a novel MgO containing PMO-IL (MgO@PMO-IL) and examined its application in the Feist–Benary reaction for the synthesis of novel spirooxindole-furan derivatives via three-component reaction of isatin derivatives with 1,3-dicarbonyl compounds and *N*-phenacyl pyridinium salts (Scheme 1). The products were synthesized under green reaction conditions with excellent yields, low reaction time and simple work-up in the presence of a highly efficient and recoverable nanocatalyst.[8]

2 | RESULTS AND DISCUSSION

With the purpose of the preparation of a novel nanocatalyst (MgO@PMO-IL) with high surface areas, uniform pore sizes, large pore volumes, high loading of organic functional groups, and good thermal and mechanical stability, we designed a method that is shown in Scheme 2.

At first, PMO-IL was prepared by hydrolysis and polymerization of tetramethoxysilane and 1,3-bis(3-trimethoxysilylpropyl) imidazolium chloride[29] using Pluronic P123 [poly (ethylene glycol)-poly (propylene glycol)-poly (ethylene glycol)] as a structure-directing agent. PMO-IL was synthesized in a simpler modified procedure compared with the last synthesis reports.[41] We used sodium imidazolide instead of imidazole and sodium hydride[21,30] and normal reaction conditions in the one-pot process (instead of absence of light condition).[42] Then, magnesium oxide nanoparticles [MgO-NPs; 20 nm diameter, specific surface area (SSA): > 60 m^2 g^{-1}] were supported on the pore walls of PMO-IL in dimethyl sulfoxide to produce MgO@PMO-IL nanocatalyst. The prepared nanocatalyst was characterized by various selected techniques, including N_2 adsorption/desorption, Fourier transform-infrared (FT-IR), thermogravimetric analysis (TGA), transmission electron microscopy (TEM) and field emission-scanning electron microscopy (FE-SEM).

FT-IR of PMO-IL (Figure 1) showed a broad peak at 3448 cm^{-1} for the O-H stretching vibration, and a peak at 2924 cm^{-1} for saturated C-H stretching. In addition, other absorption bands were observed at 1634 cm^{-1} for C=N stretching of the imidazolium ring, at 1090 and 964 cm^{-1} for asymmetric and symmetric stretching vibrations of Si-O-Si, at 799 cm^{-1} for C-Si stretching, and at 465 cm^{-1} for Si-O-Si bending vibration.

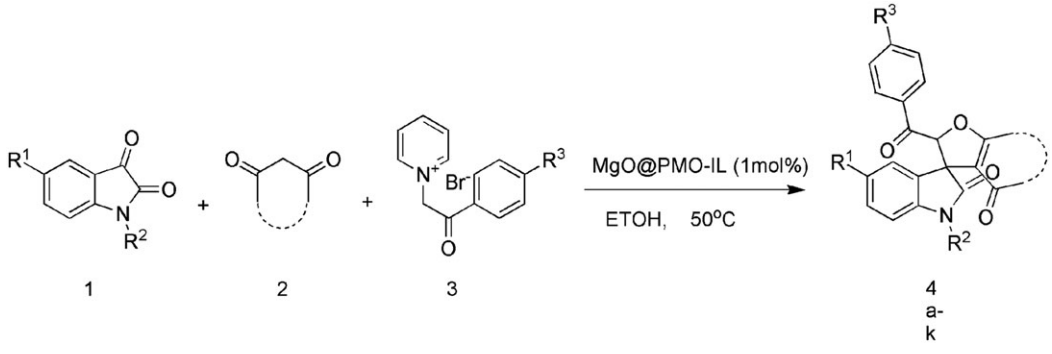

SCHEME 1 Preparation of 6-benzoyl-1,3-dimethyl-1H-spiro [furo [2,3-d]pyrimidine-5,3′-indoline]- 2,2′,4(3H,6H)-trione (**4c**) in the presence of MgO@PMO-IL

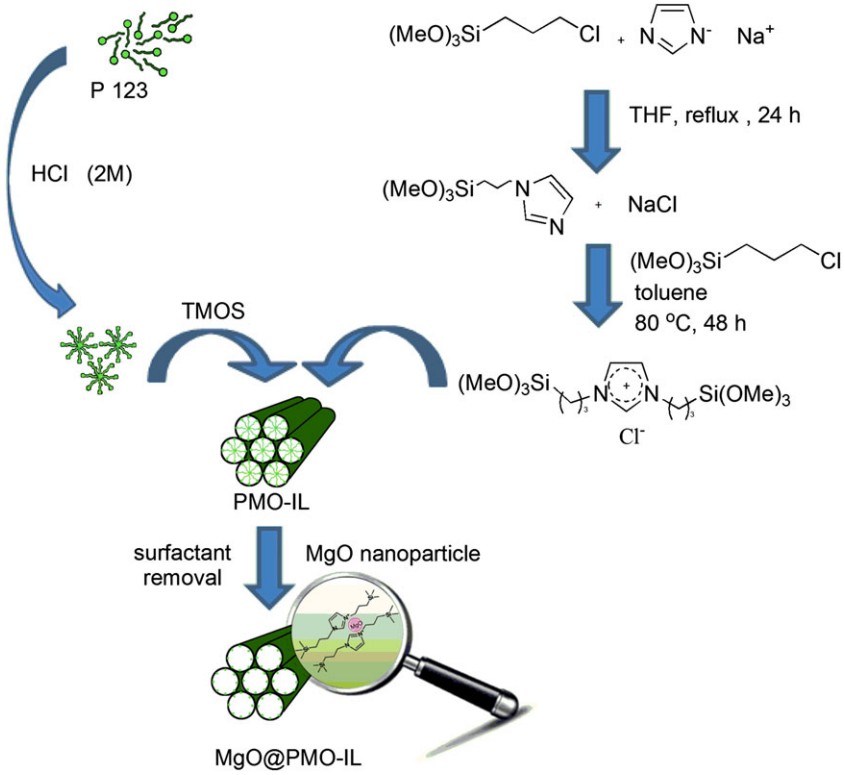

SCHEME 2 Preparation of the MgO@PMO-IL nanocatalyst

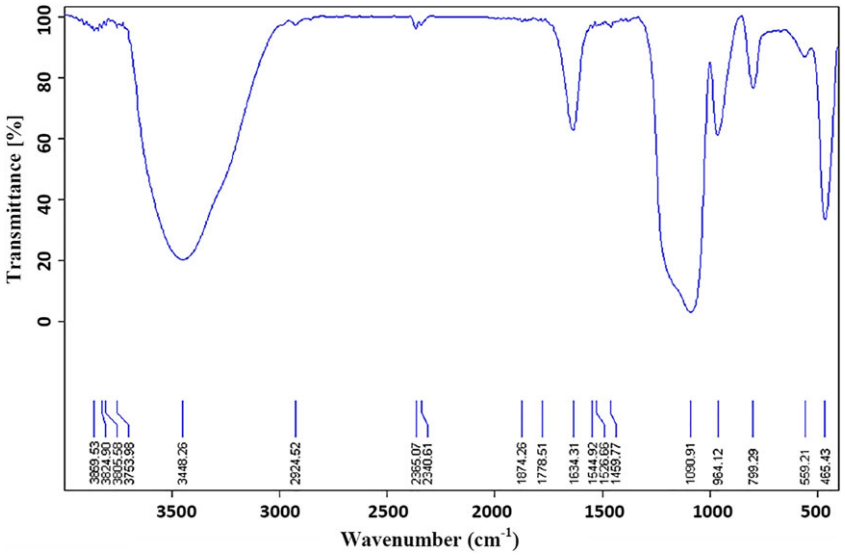

FIGURE 1 Fourier transform-infrared spectroscopy (FT-IR) of ionic liquid-based periodic mesoporous organosilica (PMO-IL)

Thermogravimetric analysis of PMO-IL (Figure 2) showed a weight loss of about 5% below 100°C related to elimination of water. Also, 2% mass loss occurring from 100 to 232°C and the main weight loss of 17% from 232 to 800°C can be attributed to the pyrolysis of P123 and IL functional groups. The results of TGA clearly demonstrate the high thermal stability of the catalyst.

As can be seen in Figure 3, N_2 adsorption–desorption analysis of PMO-IL showed a type IV isotherm with an H1 hysteresis loop, which is characteristic of mesoporous materials with a uniform pore size distribution.[23,43] Moreover, the PMO-IL displayed a high Brunauer–Emmett–Teller surface area of 623 $m^2 g^{-1}$ with a total pore volume of 1.89 $cm^3 g^{-1}$, and the Barrett–Joyner–Halenda calculations illustrated highly uniform pore diameter distribution of 5.3 nm for PMO-IL. Furthermore, decreasing SSA and pore volume of MgO@PMO-IL to 523 $m^2 g^{-1}$ and 0.80 $cm^3 g^{-1}$ clearly showed that MgO has been successfully immobilized inside the pores of the PMO-IL (see Supporting Information).

Scanning emission microscopy analysis of MgO@PMO-IL was also performed to study the

FIGURE 2 Thermogravimetric analysis (TGA) of the ionic liquid-based periodic mesoporous organosilica (PMO-IL)

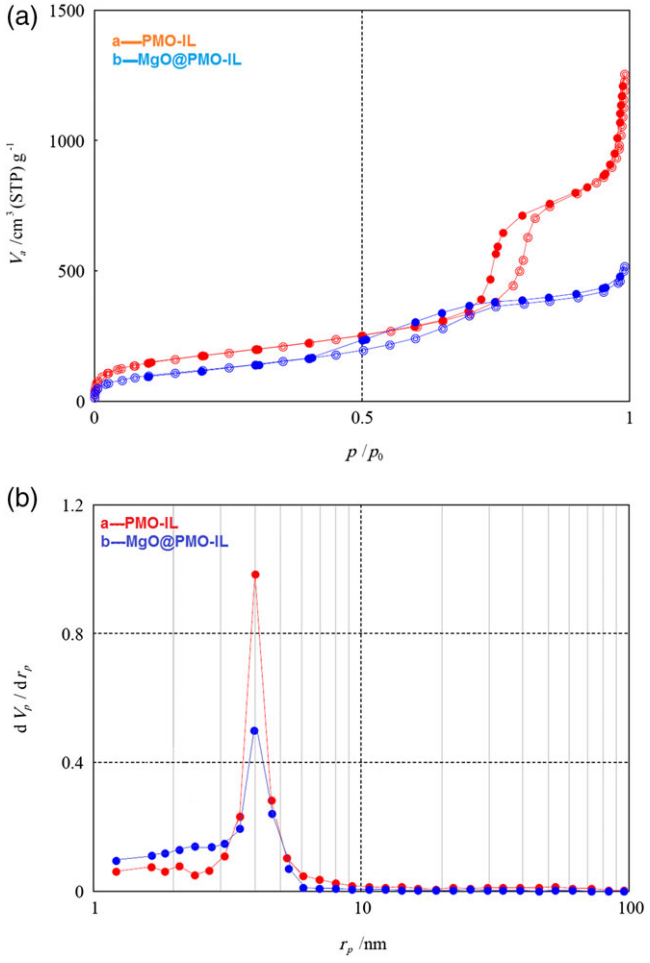

FIGURE 3 (a) N_2 adsorption–desorption; and (b) pore size distributions isotherms of ionic liquid-based periodic mesoporous organosilica (PMO-IL) and MgO@PMO-IL

morphology of the material (Figure 4a and b). These images illustrate a uniform structure. The TEM image of MgO@PMO-IL (Figure 4c) clearly showed a two-dimensional hexagonal mesostructure with a well-ordered and regular mesoporous. These SEM and TEM images were in good agreement with the data obtained from nitrogen sorption.

Finally, the MgO content in MgO@PMO-IL was determined to be 0.6 mmol g^{-1} using the induced coupled plasma (ICP) technique.

To investigate the catalytic performance of the synthesized MgO@PMO-IL, we chose the three-component reaction of 1,3-dimethyl barbituric, *N*-phenacyl pyridinium bromide and isatin as model reaction (Scheme 1), and studied different reaction parameters (Table 1). First, the model reaction in the presence of MgO@PMO-IL nanocatalyst was examined in various solvents, including tetrahydrofuran, dichloromethane, water, combination of water and ethanol (1:1), and solvent-free conditions at 50°C (Table 1, entries 1–6). It was found that ethanol gave the best result with 95% yield in 40 min. The reaction time and the product yield in the presence of MgO@PMO-IL in ethanol did not change with increasing the temperature to 78°C (Table 1, entries 6–8). The effect of catalyst amount on the reaction conditions was also explored, and it was observed that the use of 1 mol% MgO@PMO-IL is sufficient to conduct the model reaction with excellent yield in short reaction time (Table 1, entries 6, 9 and 10). Performing the model reaction with MgO[37] and PMO-IL significantly decreased the product yield and the

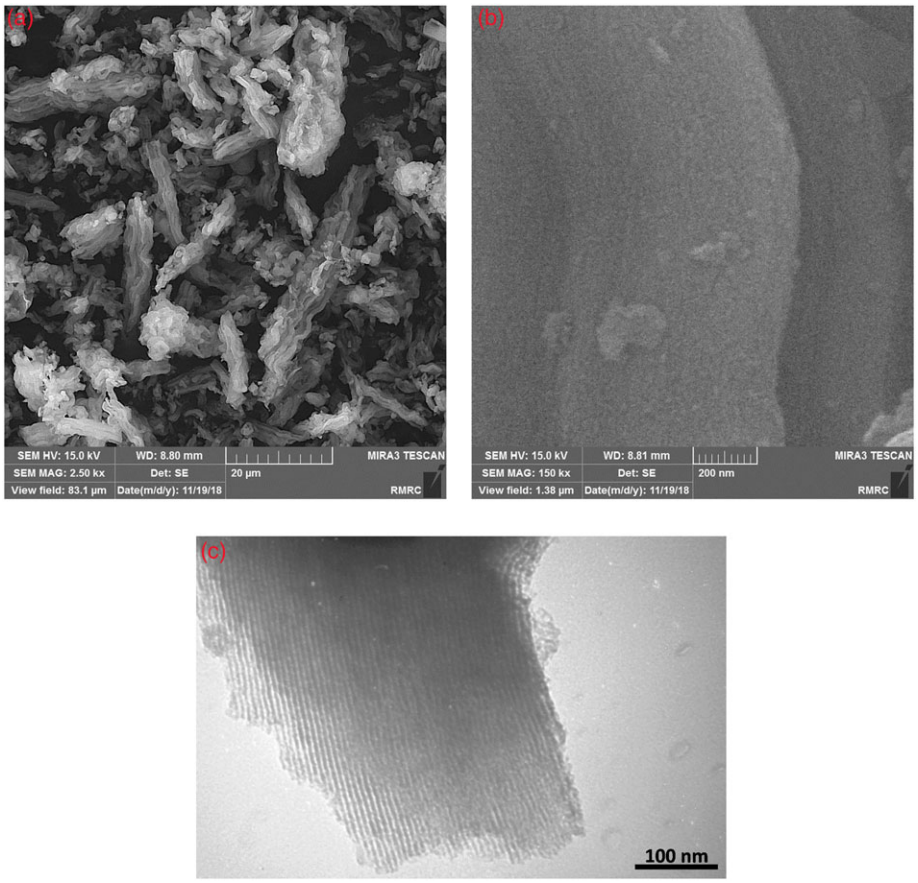

FIGURE 4 Scanning electron microscopy (SEM) images (a and b) and transmission electron microscopy (TEM) image (c) of MgO@PMO-IL catalyst

reaction rate in comparison with MgO@PMO-IL (Table 1, entries 11 and 12).

The efficiency of MgO@PMO-IL nanocatalyst was compared with different homogeneous catalysts, including K_2CO_3, DBU, DABCO and NEt_3 in ethanol at 50°C (Table 1, entries 13–16). As shown, MgO@PMO-IL gave more yield and shorter reaction time than homogenous catalysts in ethanol at 50°C (Table 1, entry 6). In addition, the reaction did not proceed in the absence of any catalyst (Table 1, entry 17). Thus, MgO@PMO-IL was selected as an optimum catalyst for the model reaction in ethanol at 50°C.

In order to expand the scope of the reaction, we used MgO@PMO-IL for the synthesis of novel spirooxindole-furan derivatives through the three-component reaction of 1,3-dicarbonyl compounds with *N*-phenacyl pyridinium salts and isatin derivatives (Table 2) under the optimized reaction conditions, and the products were obtained in high yields at short reaction times.

The structures of novel spirooxindole-furan derivatives were confirmed by FT-IR, ^{1}H-NMR, ^{13}C-NMR and mass spectroscopy (see Supporting Information). For instance, the mass spectrum of **4d** exhibited the molecular ion peak at m/z: 437, which is consistent with the molecular weight of this product. The IR spectrum of **4d** showed a broad peak at 3452 cm^{-1} corresponding to the vibration of the N-H group, and a sharp peak at 2955 cm^{-1} that is related to saturated C-H stretching. Moreover, the peaks in the region 1742–1643 cm^{-1} are related to the C=O stretching. The ^{1}H-NMR spectrum of **4d** in $CDCl_3$ showed two singlets at 3.23 and 3.57 ppm related to the two methyl groups of barbiturate acid, one doublet at 6.28 ppm ($^3J_{HH}$ = 9.2 Hz) for the CH group of oxindole, and one singlet at 6.57 ppm associated to the CH group of the furan ring. The aromatic protons appeared as three multiplets at about 6.90–6.93, 7.26–7.30 and 7.44–7.47 ppm. The NH proton of oxindole appeared as one broad singlet at 8.95 ppm. The proton-decoupled ^{13}C-NMR spectrum of **4d** showed 22 distinct resonances in agreement with the proposed structure, including two signals at 27.9 and 30.1 ppm for N-CH_3, and two signals at 58.8 and 91.1 ppm for the spiro carbon atom and the furan carbon atom, respectively.

A plausible mechanism is illustrated in Scheme 3, which is supported by the previous literature.[8,40]

To evaluate the recoverability and reusability of MgO@PMO-IL, we used this catalyst in the three-

TABLE 1 Optimization for the three-component reaction of 1,3-dimethyl barbituric, *N*-phenacyl pyridinium bromide and isatin[a]

Entry	Catalyst (mol%)	Solvent	Temp. (°C)	Time	Yield (%)
1	MgO@PMO-IL (1)	DCM	50	8 hr	65
2	MgO@PMO-IL (1)	H_2O	50	6 hr	65
3	MgO@PMO-IL (1)	H_2O-Ethanol (1:1)	50	5 hr	70
4	MgO@PMO-IL (1)	THF	50	8 hr	50
5	MgO@PMO-IL (1)	–	50	10 hr	60
6	MgO@PMO-IL (1)	EtOH	50	40 min	95
7	MgO@PMO-IL (1)	EtOH	25	8 hr	70
8	MgO@PMO-IL (1)	EtOH	78	40 min	96
9	MgO@PMO-IL (0.7)	EtOH	50	40 min	70
10	MgO@PMO-IL (1.5)	EtOH	50	40 min	96
11	PMO-IL (1)	EtOH	50	6 hr	25
12	MgO (1)	EtOH	50	2 hr	80
13	K_2CO_3 (1)	EtOH	50	15 hr	45
14	DBU (1)	EtOH	50	15 hr	60
15	DABCO (1)	EtOH	50	18 hr	65
16	NEt_3 (1)	EtOH	50	10 hr	85
17	–	EtOH	50	24 hr	–

[a]Reaction conditions: 1,3-dimethyl barbituric acid (1 mmol), *N*-phenacyl pyridinium bromide (1 mmol) and isatin (1 mmol).

component reaction of 1,3-dimethyl barbituric, *N*-phenacyl pyridinium bromide and isatin under the optimized conditions. The catalyst was recovered through a simple filtration process and reused for at least seven times without a significant decrease in its catalytic activity (Figure 5).

The FT-IR analysis of the recovered catalyst (Figure 6) showed that the stability of IL units during reaction conditions was in good agreement with the data achieved from the recoverability of the nanocatalyst.

3 | CONCLUSION

In conclusion, with the aim of preparing a novel nanocatalyst, the supported nano-MgO on PMO-IL (MgO@PMO-IL) with uniform pore size, large pore volumes, high surface areas, high loading of organic functional groups and good thermal stability was synthesized and then characterized by N_2 adsorption/desorption, FT-IR, TEM, FE-SEM, TGA and ICP analyses. The catalytic performance of MgO@PMO-IL was investigated in the synthesis of novel spirooxindole-furan derivatives through the three-component reaction of 1,3-dicarbonyl compounds, *N*-phenacyl pyridinium salts and isatin derivatives. These products were prepared under mild reaction conditions with good yields, short reaction times and a simple work-up procedure. In addition, the catalyst was recovered and reused for at least seven times without a significant decrease in its catalytic activity.

4 | EXPERIMENTAL

All of the chemicals and solvents were purchased from Merck and Aldrich without need for further purification. The progress of the reactions was monitored by thin-layer chromatography (TLC) using silica gel SIL G/UV 254 plates. Melting points were measured on an Electrothermal 9100 apparatus and are uncorrected. IR spectra (KBr) were recorded on a FT-IR BRUKER VECTOR 22 spectrometer. ^{1}H- and ^{13}C-NMR spectra were measured with Bruker DRX-400 Avance instrument (400.13 and 100.61 MHz, respectively), and Bruker Avance 300 NMR (300.13 and 75.46 MHz, respectively) in $CDCl_3$ and (D6) DMSO. Mass spectra were recorded on a Finnigan-Matt 8430 mass spectrometer operating at an ionization potential of 70 eV. The TGA was measured by BAHR-Thermoanalyse (GmbH STA 503) from room temperature to 800°C. The size and structure of the materials were shown using TEM (Zeiss-EM10C-100 kV), FE-SEM

TABLE 2 Synthesis of novel spirooxindole-furan derivatives in the presence of MgO@PMO-Il[a]

Entry	R^1	R^2	R^3	1-3-Dicarbonyl compound	Product	Time (min)	m.p. (°C)	Yield (%)
1	H	H	H	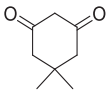	**4a**	40	275–276 (275–277)[b]	90
2	Cl	H	H	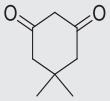	**4b**	40	261–263 (260–263)[b]	95
3	H	H	H	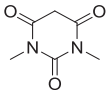	**4c**	40	244–248 (245–247)[b]	95
4	Cl	H	H	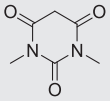	**4d**	30	297–300	97
5	H	CH_3	H	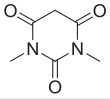	**4e**	50	216–218	90
6	Cl	CH_2CO_2Et	H	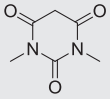	**4f**	30	213–215	95
7	H	$PhCH_2$	H	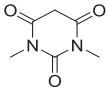	**4 g**	30	261–263	97
8	H	$CH_2CO_2CH_3$	H	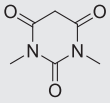	**4 h**	30	225–227	97
9	H	$CH_2C \equiv CH$	H	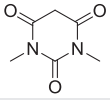	**4i**	30	261–263	97
10	H	H	F	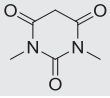	**4j**	30	229–231	95
11	Cl	H	F	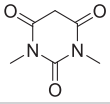	**4 k**	30	322–324	95

[a]Reaction conditions: 1,3-dicarbonyl compound (1 mmol), *N*-phenacyl pyridinium salt (1 mmol) and isatin derivatives (1 mmol), MgO@PMO-IL (1 mol%), EtOH (5 mL), 50°C, stirring.

[b]Reported m.p.

(MIRA3 XMU), and were verified further by N_2 adsorption/desorption analysis [BELsorp-max (Japan)]. The ICP technique was determined by VARIAN VISTA-PRO instrument.

4.1 | Synthesis of imidazolium ionic liquid

The IL was prepared according to the previously reported procedures with a few modifications.[30,35,42] Typically, sodium imidazolide (0.5 g) and 3-chloropropyltrimethoxysilane (1.35 mL) were added to a well-dried two-necked flask containing dry THF (20 mL). The mixture was stirred under reflux conditions for 24 hr under argon atmosphere. Then it was cooled to room temperature and the solvent was removed under reduced pressure. Thereafter, 3-chloropropyltrimethoxysilane (1.35 mL) and dry toluene (20 mL) were added, and the mixture was heated at 80°C for 48 hr. The toluene phase was removed, and then dry CH_2Cl_2 was added to precipitate NaCl. The CH_2Cl_2 phase was transferred to another flask, and CH_2Cl_2 was removed under reduced pressure.

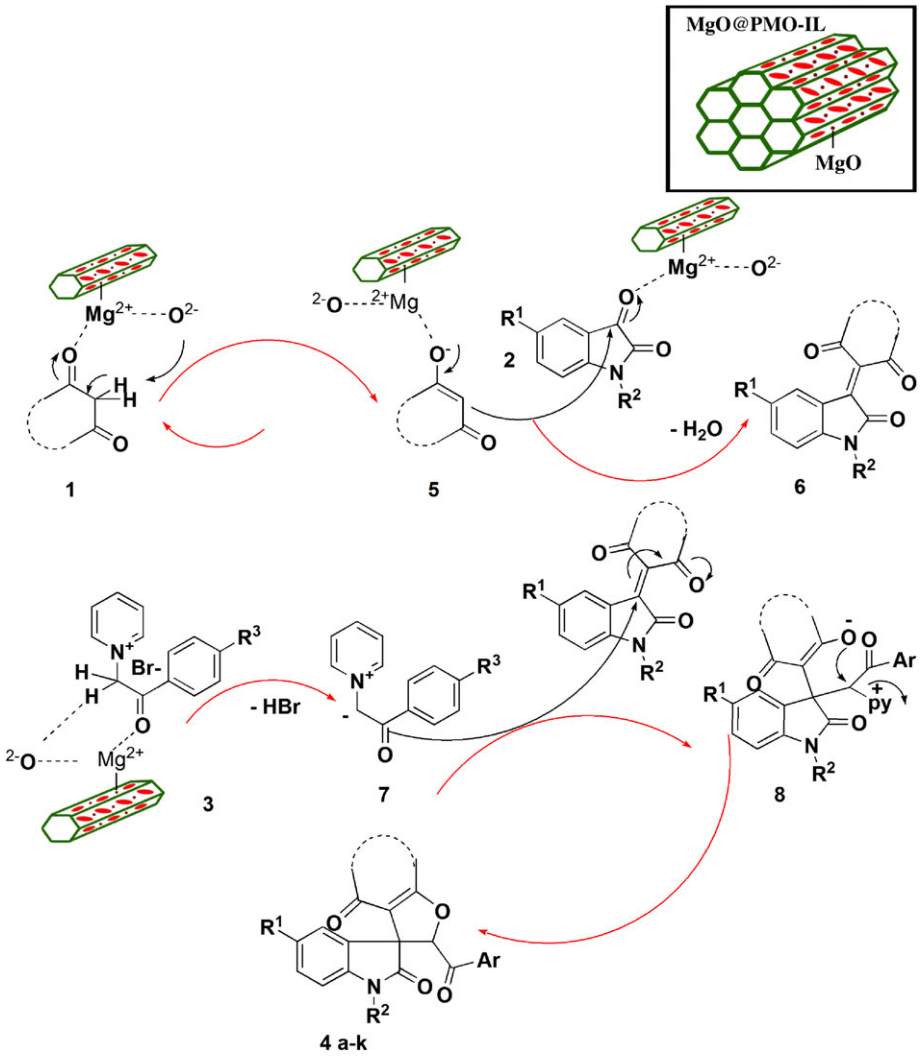

SCHEME 3 Proposed mechanism for the preparation of spirooxindole-furan derivatives using MgO@PMO-IL as heterogenous nanocatalyst

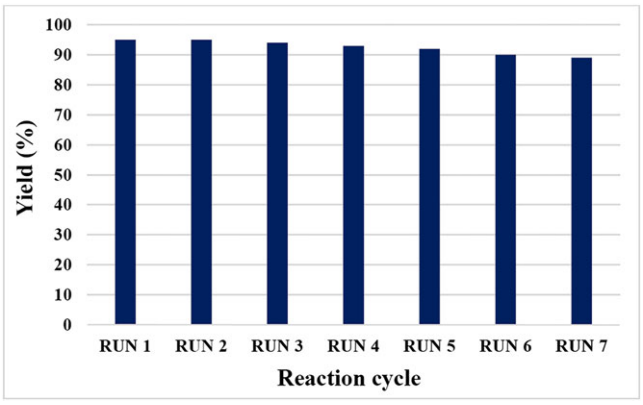

FIGURE 5 Recyclability test of MgO@PMO-IL during the three-component reaction of 1,3- dimethyl barbituric acid with *N*-phenacyl pyridinium bromide and isatin in the presence of MgO@PMO-IL in ethanol at 50°C

Finally, the obtained viscous yellow product was washed with dry toluene several times.

4.2 | Synthesis of PMO-IL

The PMO-IL was synthesized according to the last reported literature.[30,35,42] P123 (1.67 g), KCl (8.8 g), HCl (2 M, 46.14 g) and distilled H_2O (10.5 g) were mixed and stirred at 40°C until a homogenous solution was obtained. Then IL (0.86 g) and a solution of tetramethoxysilane (2.74 g) in dry methanol were added to the mixture and stirred at 40°C for 24 hr, then it was aged at 100°C for 48 hr. Thereafter, the mixture was cooled to room temperature and washed with deionized water. The surfactant was extracted by a Soxhlet extractor

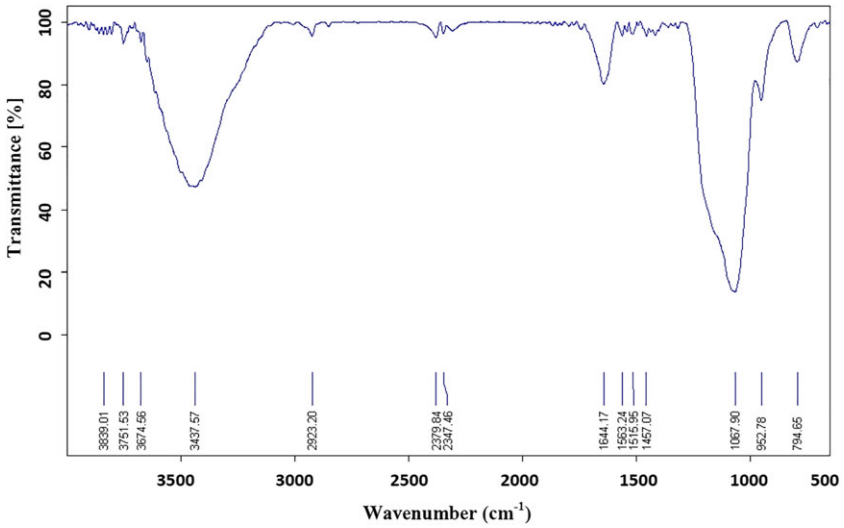

FIGURE 6 Fourier transform-infrared (FT-IR) analysis of the recovered MgO@PMO-IL

using ethanol (100 mL) and HCl (3 mL) for each 1 g of PMO-IL for six times over 12 hr. Finally, PMO-IL was dried at 50°C in vacuum.

4.3 | Synthesis of MgO@PMO-IL

First, PMO-IL (0.2 g) was dispersed in DMSO (1 mL). Then, nano-MgO (0.1 mmol) was added and the mixture was stirred at 50°C for 6 hr, and then at 100°C for 2 hr. Subsequently, the mixture was cooled to room temperature and washed with ethanol several times and dried at 60°C for 12 hr.

4.4 | General procedure for the synthesis of compounds 4a–k

A mixture of 1,3-dicarbonyl compounds (1 mmol), isatin (1 mmol) and *N*-phenacyl pyridinium bromide (1 mmol) in ethanol (5 mL) in the presence of MgO@PMO-IL (1 mol%) as catalyst was stirred at 50°C for the specified time period. The reaction was monitored by TLC (EtOAc/*n*-hexane, 1:1). After completion of the reaction, the solvent was evaporated under reduced pressure and the product was obtained by recrystallization from methanol.

4.5 | Physical and spectral data for compounds 4a–k

4.5.1 | 2-Benzoyl-6,6-dimethyl-6,7-dihydro-2H-spiro [benzofuran-3,3′-indoline]-2′,4(5H)-dione (4a)

White powder, m.p.: 275–276°C; yield (0.34 g, 90%); IR (KBr) (ν_{max}, cm^{-1}): 3430 (NH), 2939 (C_{sp3}-H), 1725–1645 (C=O), 1476 (C=C), 1257 (C_{sp2} -O), 1065 (C_{sp3}-O); ^{1}H-NMR (400 MHz, $CDCl_3$), δ_H (ppm): 1.15 and 1.22 (2 s, 6H, $2CH_3$), 2.13 and 2.31 (2d, 2H, $^2J_{HH}$ = 16.4 Hz, AB-system, CH_2), 2.64 and 2.70 (2d, 2H, $^2J_{HH}$ = 18.0 Hz, AB-system, CH_2), 6.46 (d, 1H, $^3J_{HH}$ = 7.6 Hz, $CH_{Oxindole}$), 6.47 (s, 1H, CH_{furan}), 6.87–6.88 (m, 2H, $2CH_{Ar}$), 6.97–7.01 (m, 1H, CH_{Ar}), 7.23–7.28 (m, 2H, $2CH_{Ar}$), 7.40–7.45 (m, 3H, $3CH_{Ar}$), 7.79 (br s, 1H, NH); ^{13}C-NMR (100 MHz, $CDCl_3$), δ_C (ppm): 27.7 and 29.4 ($2CH_3$), 34.5 (CMe_2), 37.7 and 50.8 ($2CH_2$), 58.9 (C_{spiro}), 91.4 (CH_{furan}), 109.6 (CH_{Ar}), 114.5 (Cq), 122.9 and 124.8 ($2CH_{Ar}$), 126.5 (Cq), 127.5 and 128.5 ($4CH_{Ar}$), 129.1 and 133.7 ($2CH_{Ar}$), 134.6, 139.6 and 177.3 (3Cq), 178.1 (CO_{amide}), 192.2 and 192.3 ($2CO_{ketone}$); MS, m/z: 387 ($M^{+\bullet}$).

4.5.2 | 2-Benzoyl-5′-chloro-6,6-dimethyl-6,7-dihydro-2H-spiro [benzofuran-3,3′-indoline]-2′,4(5H)-dione (4b)

White powder, m.p.: 261–263°C; yield (0.40 g, 95%); IR (KBr) (ν_{max}, cm^{-1}): 3291 (NH), 2958 (C_{sp3}-H), 1727–1644 (C=O), 1223 (C_{sp2} = O), 1065 (C_{sp3} = O); ^{1}H-NMR (400 MHz, $CDCl_3$), δ_H (ppm): 1.20 and 1.30 (2 s, 6H, $2CH_3$), 2.17 and 2.30 (2d, 2H, $^2J_{HH}$ = 16.4 Hz, AB-system, CH_2), 2.64 and 2.71 (2d, 2H, $^2J_{HH}$ = 18.0 Hz, AB-system, CH_2), 6.40 (d, 1H, $^3J_{HH}$ = 8.4 Hz, $CH_{Oxindole}$), 6.46 (s, 1H, CH_{furan}), 6.85 (d, 1H, $^4J_{HH}$ = 2.4 Hz, CH_{Ar}), 6.97 (dd, 1H, $^3J_{HH}$ = 8.4 Hz, $^4J_{HH}$ = 2.0 Hz, CH_{Ar}), 7.27–7.31 (m, 2H, $2CH_{Ar}$), 7.44–7.48 (m, 3H, $3CH_{Ar}$), 7.77 (br s, 1H, NH); ^{13}C-NMR (100 MHz, $CDCl_3$), δ_C (ppm): 28.0 and 29.2 ($2CH_3$), 34.5 (CMe_2), 37.7 and 50.8 ($2CH_2$), 58.9 (C_{spiro}), 91.2 (CH_{furan}), 110.6 (CH_{Ar}), 114.3 (Cq), 125.1 and 127.6 ($4CH_{Ar}$), 128.2 and 128.3 (2Cq), 128.7, 129.1 and 133.9 ($3CH_{Ar}$), 134.5, 138.3 and 176.9 (3Cq), 178.6 (CO_{amide}), 191.9 and 192.3 ($2CO_{ketone}$); MS, m/z: 423 and 421 ($M^{+\bullet}$).

4.5.3 | 6-Benzoyl-1,3-dimethyl-1H-spiro [furo [2,3-d]pyrimidine-5,3′-indoline]-2,2′,4(3H,6H)-trione (4c)

White powder, m.p.: 244–248°C; yield (0.38 g, 95%); IR (KBr) (ν_{max}, cm^{-1}): 3430 (NH), 2925 (C_{sp3}-H), 1709–1646 (C=O), 1190 (C_{sp2}-O), 1111 (C_{sp3}-O); ^{1}H-NMR (400 MHz, $CDCl_3$), δ_H (ppm): 3.23 and 3.58 (2 s, 6H, 2 N-CH_3), 6.48 (d, 1H, $^3J_{HH}$ = 7.6 Hz, $CH_{Oxindole}$), 6.60 (s, 1H, CH_{furan}), 6.90 (td, 1H, $^3J_{HH}$ = 7.6 Hz, $^4J_{HH}$ = 0.8 Hz, CH_{Ar}), 6.94 (td, 1H, $^3J_{HH}$ = 8.0 Hz, $^4J_{HH}$ = 0.8 Hz, CH_{Ar}), 7.01 (td, 1H, $^3J_{HH}$ = 7.6 Hz, $^4J_{HH}$ = 1.6 Hz, CH_{Ar}), 7.25–7.29 (m, 2H, $2CH_{Ar}$),7.42–7.47 (m, 3H, $3CH_{Ar}$), 7.97 (br s, 1H, NH); ^{13}C-NMR (100 MHz, $CDCl_3$), δ_C (ppm): 27.9 and 30.1 ($2CH_3$), 58.8 (C_{spiro}), 91.1 (CH_{furan}), 109.9 and 123.2 ($2CH_{Ar}$), 125.4 and 125.6 (2Cq), 127.5 and 128.7 ($4CH_{Ar}$), 129.6 and 134.1 ($2CH_{Ar}$), 139.7 (Cq), 148.0 (CH_{Ar}), 151.4 and 158.1 (2Cq), 163.2, 176.9 and 179.8 ($3CO_{amide}$), 190.6 (CO_{ketone}); MS, m/z: 403 ($M^{+\bullet}$).

4.5.4 | 6-Benzoyl-5′-chloro-1,3-dimethyl-1H-spiro [furo [2,3-d]pyrimidine-5,3′-indoline]-2,2′,4(3H,6H)-trione (4d)

White powder, m.p.: 297–300°C; yield (0.42 g, 97%); IR (KBr) (ν_{max}, cm^{-1}): 3452 (NH), 2955 (C_{sp3}-H), 1742–1643 (C=O), 1255 (C_{sp2}-O), 1182 (C_{sp3}-O); ^{1}H-NMR (400 MHz, $CDCl_3$), δ_H (ppm): 3.24 and 3.58 (2 s, 6H, 2 N-CH_3), 6.28 (d, 1H, $^3J_{HH}$ = 9.2 Hz, $CH_{Oxindole}$), 6.57 (s, 1H, CH_{furan}), 6.90–6.93 (m, 2H, $2CH_{Ar}$), 7.26–7.30 (m, 2H, $2CH_{Ar}$), 7.44–7.47 (m, 3H, $3CH_{Ar}$), 8.95 (br s, 1H, NH); ^{13}C-NMR (100 MHz, $CDCl_3$), δ_C (ppm): 28.0 and 30.2 ($2CH_3$), 58.5 (C_{spiro}), 89.0 (Cq), 91.1 (CH_{furan}), 111.2. and 125.4 ($2CH_{Ar}$), 127.2 (Cq), 127.6 ($2CH_{Ar}$), 128.3 (Cq), 128.8 ($2CH_{Ar}$), 129.6 (CH_{Ar}), 133.9 (Cq), 134.2 (CH_{Ar}), 138.9 and 151.0 (2Cq), 158.5, 163.5 and 176.4 ($3CO_{amide}$), 190.2 (CO_{ketone}); MS, m/z: 437 ($M^{+\bullet}$).

4.5.5 | 6-Benzoyl-1,1′,3-trimethyl-1H-spiro [furo [2,3-d]pyrimidine-5,3′-indoline]-2,2′,4(3H,6H)-trione (4e)

White powder, m.p.: 233–237°C; yield (0.40 g, 97%); IR (KBr) (ν_{max}, cm^{-1}): 3520 (NH), 2937 (C_{sp3}-H), 1722–1612 (C=O), 1261 (C_{sp2}-O), 1194 (C_{sp3}-O); ^{1}H-NMR (400 MHz, $CDCl_3$), δ_H (ppm): 3.10, 3.20 and 3.58 (3 s, 9H, 3 N-CH_3), 6.42 (d, 1H, $^3J_{HH}$ = 8.0 Hz, $CH_{Oxindole}$), 6.58 (s, 1H, CH_{furan}), 6.92–6.98 (m, 2H, $2CH_{Ar}$), 7.08 (td, 1H, $^3J_{HH}$ = 6.4 Hz, $^4J_{HH}$ = 2 Hz, CH_{Ar}), 7.22–7.25 (m, 2H, $2CH_{Ar}$), 7.28–7.31 (m, 2H, $2CH_{Ar}$), 7.49 (m, 1H, CH_{Ar}); ^{13}C-NMR (100 MHz, $CDCl_3$), δ_C (ppm): 26.8 and 27.9, 30.1 ($3CH_3$), 58.3 (C_{spiro}), 89.0 (Cq), 91.7 (CH_{furan}), 108.1, 123.2 and 124.8 ($3CH_{Ar}$), 125.2 (Cq), 127.4 and 128.4 ($4CH_{Ar}$), 129.7 and 133.8 ($2CH_{Ar}$), 134.2, 142.5 and 151.3 (3Cq), 158.0, 163.1 and 175.3 ($3CO_{amide}$), 190.7 (CO_{ketone}); MS, m/z: 417 ($M^{+\bullet}$).

4.5.6 | Ethyl 2-(6-benzoyl-5′-chloro-1,3-dimethyl-2,2′,4-trioxo-2,3,4,6-tetrahydro-1H-spiro [furo[2,3-d]pyrimidine-5,3′-indolin]-1′-yl) acetate (4f)

White powder, m.p.: 216–218°C; yield (0.50 g, 95%); IR (KBr) (ν_{max}, cm^{-1}): 3434 (NH), 2924 (C_{sp3}-H), 1746–1613 (C=O), 1216 (C_{sp2}-O), 1175 (C_{sp3}-O); ^{1}H-NMR (400 MHz, $CDCl_3$), δ_H (ppm): 1.33 (t, 3H, $^3J_{HH}$ = 7.2 Hz, CH_3), 3.21 and 3.57 (2 s, 6H, 2 N-CH_3), 4.27 (m, 2H, OCH_2), 4.28 and 4.63 (2d, 2H, $^2J_{HH}$ = 17.6 Hz, AB-system, N-CH_2), 6.43 (d, 1H, $^3J_{HH}$ = 8.4 Hz, $CH_{Oxindole}$), 6.57 (s, 1H, CH_{furan}), 6.94 (d, 1H, $^4J_{HH}$ = 2.0 Hz, CH_{Ar}), 7.037 (dd, 1H, $^3J_{HH}$ = 8.4 Hz, $^4J_{HH}$ = 2.0 Hz, CH_{Ar}), 7.35 (t, 2H, $^3J_{HH}$ = 7.6 Hz, $2CH_{Ar}$), 7.48 (t, 1H, $^3J_{HH}$ = 7.6 Hz, $2CH_{Ar}$), 7.56 (d, 2H, $^3J_{HH}$ = 8.8 Hz, $2CH_{Ar}$); ^{13}C-NMR (100 MHz, $CDCl_3$), δ_C (ppm): 14.2, 27.9 and 30.1 ($3CH_3$), 42.0 (N-CH_2), 58.1 (C_{spiro}), 62.0 (CH_2), 88.7 (Cq), 89.9 (CH_{furan}), 109.3 and 125.8 ($2CH_{Ar}$), 126.4 (Cq), 127.9 ($2CH_{Ar}$), 129.0 (Cq), 129.1 ($2CH_{Ar}$), 129.6 (CH_{Ar}), 133.7 (Cq), 134.3 (CH_{Ar}), 140.4 and 151.2 (2Cq), 157.9 (CO_{ester}), 163.5, 166.7 and 175.4 ($3CO_{amide}$), 190.0 (CO_{ketone}); MS, m/z: 523 ($M^{+\bullet}$).

4.5.7 | 6-Benzoyl-1′-benzyl-1,3-dimethyl-1H-spiro [furo[2,3-d]pyrimidine-5,3′-indoline]-2,2′,4(3H,6H)-trione (4g)

White powder, m.p.: 213–215°C; yield (0.48 g, 97%); IR (KBr) (ν_{max}, cm^{-1}): 3434 (NH), 2926 (C_{sp3}-H), 1722–1665 (2C=O), 1216 (C_{sp2}-O), 1175 (C_{sp3}-O); ^{1}H-NMR (400 MHz, $CDCl_3$), δ_H (ppm): 3.24 and 3.59 (2 s, 6H, 2 N-CH_3), 4.55 and 5.11(2d, 2H, $^2J_{HH}$ = 16 Hz, AB-system, N-CH_2), 6.31 (d, 1H, $^3J_{HH}$ = 7.6 Hz, $CH_{Oxindole}$), 6.64 (s, 1H, CH_{furan}), 6.87–6.91 (m, 1H, CH_{Ar}), 6.94–6.99 (m, 2H, $2CH_{Ar}$), 7.13–7.17 (m, 2H, $2CH_{Ar}$), 7.27–7.36 (m, 7H, $2CH_{Ar}$), 7.41–7.46 (m, 1H, CH_{Ar}); ^{13}C-NMR (100 MHz, $CDCl_3$), δ_C (ppm): 28.0 and 30.1 (2 N-CH_3), 44.6 (N-CH_2), 58.3 (C_{spiro}), 89.4 (Cq), 91.1 (CH_{furan}), 109.3 and 123.3 ($2CH_{Ar}$), 125.1 and 125.2 (2Cq), 127.1 and 127.5 ($4CH_{Ar}$), 127.6 (Cq), 128.6 and 128.9 ($4CH_{Ar}$), 129.5 and 133.9 ($2CH_{Ar}$), 134.2 and 134.7 (2Cq), 141.9 and 151.3 (2Cq), 157.9, 163.0 and 175.6 ($3CO_{amide}$), 190.7 (CO_{ketone}); MS, m/z: 493 ($M^{+\bullet}$).

4.5.8 | Methyl 2-(6-benzoyl-1,3-dimethyl-2,2′,4-trioxo-2,3,4,6-tetrahydro-1H-spiro [furo[2,3-d]pyrimidine-5,3′-indolin]-1′-yl) acetate (4h)

White powder, m.p.: 225–227°C; yield (0.46 g, 97%); IR (KBr) (ν_{max}, cm^{-1}): 3442 (NH, OH), 2924 (C_{sp3}-H), 1755–1662 (C=O), 1262 (C_{sp2}-O), 11 203 (C_{sp3}-O); ^{1}H-NMR (400 MHz, $CDCl_3$), δ_H (ppm): 3.21 and 3.58 (2 s, 6H, 2 N-CH_3), 3.83 (s, 3H, OCH_3), 4.35–4.65 (2d, 2H, $^2J_{HH}$ = 17.6 Hz, AB-system, N-CH_2), 6.50 (d, 1H, $^3J_{HH}$ = 7.6 Hz, $CH_{Oxindole}$), 6.58 (s, 1H, CH_{furan}), 6.89 (td, 1H, $^3J_{HH}$ = 7.6 Hz, $^4J_{HH}$ = 0.8 Hz, CH_{Ar}), 6.97 (dd, 1H, $^3J_{HH}$ = 7.6 Hz, $^4J_{HH}$ = 0.8 Hz, CH_{Ar}), 7.07 (td, 1H, $^3J_{HH}$ = 7.6 Hz, $^4J_{HH}$ = 1.2 Hz, CH_{Ar}), 7.33–7.34 (m, 2H, $2CH_{Ar}$), 7.46 (m, 1H, CH_{Ar}), 7.52–7.54 (m, 2H, $2CH_{Ar}$); ^{13}C-NMR (100 MHz, $CDCl_3$), δ_C (ppm): 27.9 and 30.1 ($2CH_3$), 41.8 (N-CH_2), 52.8 (OCH_2), 57.1 (C_{spiro}), 83.7 (Cq), 90.2 (CH_{furan}), 108.3 and 123.6 ($2CH_{Ar}$), 124.7 (Cq), 125.4 (CH_{Ar}), 127.8 and 128.9 ($4CH_{Ar}$), 129.7 (CH_{Ar}), 133.7 (Cq), 134.1 (CH_{Ar}), 141.8 and 151.6 (2Cq), 154.8 (CO_{acid}), 157.9, 167.5 and 176.2 ($3CO_{amide}$), 190.4 (CO_{ketone}); MS, m/z: 475 ($M^{+\bullet}$).

4.5.9 | 6-Benzoyl-1,3-dimethyl-1′-(prop-2-yn-1-yl)-1H-spiro [furo[2,3-d]pyrimidine-5,3′-indoline]-2,2′,4(3H,6H)-trione (4i)

White powder, m.p.: 261–263°C; yield (0.43 g, 97%); IR (KBr) (ν_{max}, cm^{-1}): 3443 (NH), 2924 (C_{sp3}-H), 1710–1613 (C=O), 1262 (C_{sp2}-O), 1186 (C_{sp3}-O); ^{1}H-NMR (400 MHz, $CDCl_3$), δ_H (ppm): 2.23 (t, 1H, $^4J_{HH}$ = 2.4 Hz, CH_{alkin}), 3.20 and 3.57 (2 s, 6H, 2 N-CH_3), 4.31 and 4.70 (2d, 2H, $^3J_{HH}$ = 7.6 Hz, $^4J_{HH}$ = 2.4 Hz, AB-system, $2CH_{Oxindole}$), 6.60 (s, 1H, CH_{furan}), 6.74 (d, 1H, $^2J_{HH}$ = 8 Hz, CH_{Ar}), 6.92–6.99 (m, 2H, CH_{Ar}), 7.19 (td, 1H, $^3J_{HH}$ = 7.6 Hz, $^4J_{HH}$ = 1.6 Hz, CH_{Ar}), 7.24–7.26 (m, 2H, $2CH_{Ar}$), 7.36–7.38 (m, 2H, $2CH_{Ar}$), 7.40–7.44 (m, 1H, CH_{Ar}); ^{13}C-NMR (100 MHz, $CDCl_3$), δ_C (ppm): 27.9 and 30.1 ($2CH_3$), 30.1 (CH), 58.2 (C_{spiro}), 72.8 (C_{alkin}), 76.0 (Cq), 89.1 (Cq), 90.9 (CH_{furan}), 109.2 and 123.6 ($2CH_{Ar}$), 125.0 and 125.1 (2Cq), 127.3 and 128.8 ($4CH_{Ar}$), 129.6 and 134.0 ($2CH_{Ar}$), 138.3 and 140.8 (2Cq), 151.2 (Cq), 157.9, 163.1 and 174.6 ($3CO_{amide}$), 190.4 (CO_{ketone}); MS, m/z: 441 ($M^{+\bullet}$).

4.5.10 | 6-(4-fluorobenzoyl)-1,3-Dimethyl-1H-spiro [furo[2,3-d]pyrimidine-5,3′-indoline]-2,2′,4(3H,6H)-trione (4j)

White powder, m.p.: 229–231°C; yield (0.40 g, 95%); IR (KBr) (ν_{max}, cm^{-1}): 3454 (NH), 2924 (C_{sp3}-H), 1738–1598 (C=O), 1259 (C_{sp2}-O), 1230 (C_{sp3}-O); ^{1}H-NMR (400 MHz, $CDCl_3$), δ_H (ppm): 3.23 and 3.56 (2 s, 6H, 2 N-CH_3), 6.47 (d, 1H, $^3J_{HH}$ = 7.7 Hz, $CH_{Oxindole}$), 6.53 (s, 1H, CH_{furan}), 6.86–7.03 (m, 5H, CH_{Ar}), 7.56 (dd, 2H, $^3J_{HH}$ = 9.0 Hz, $^4J_{HH}$ = 6 Hz, CH_{Ar}), 8.50 (br s, 1H, NH); ^{13}C-NMR (100 MHz, $CDCl_3$), δ_C (ppm): 28.0 and 30.1 ($2CH_3$), 58.6 (C_{spiro}), 89.3 (Cq), 90.1 (CH_{furan}), 110.3, 123.1 and 125.2 ($5CH_{Ar}$), 125.4 (Cq), 129.7 (CH_{Ar}), 130.2 and 130.3 ($2CH_{Ar}$), 130.5 (Cq), 140.0 (CH_{Ar}), 151.1 (Cq), 158.3, 163.2 and 176.9 ($3CO_{amide}$), 189.0 (CO_{ketone}); MS, m/z: 421 ($M^{+\bullet}$).

4.5.11 | 5′-Chloro-6-(4-fluorobenzoyl)-1,3-dimethyl-1H-spiro [furo[2,3-d]pyrimidine-5,3′-indoline]-2,2′,4(3H,6H)-trione (4k)

White powder, m.p.: 322–324°C; yield (0.43 g, 95%); IR (KBr) (ν_{max}, cm^{-1}): 3447 (NH), 2922 (C_{sp3}-H), 1741–1598 (C=O), 1233 (C_{sp2}-O), 1202 (C_{sp3}-O); ^{1}H-NMR (400 MHz, $CDCl_3$), δ_H (ppm): 3.24 and 3.57 (2 s, 6H, 2 N-CH_3), 6.38 (d, 1H, $^3J_{HH}$ = 8.3 Hz, $CH_{Oxindole}$), 6.52 (s, 1H, CH_{furan}), 6.92–6.92 (d, 1H, $^3J_{HH}$ = 3 Hz, CH_{Ar}), 6.97–7.00 (m, 3H, $3CH_{Ar}$), 7.50 (dd, 2H, $^3J_{HH}$ = 9.0 Hz, $^4J_{HH}$ = 6 Hz, CH_{Ar}), 8.54 (br s, 1H, NH); ^{13}C-NMR (100 MHz, DMSO and $CDCl_3$), δ_C (ppm): 27.1 and 29.4 ($2CH_3$), 58.0 (C_{spiro}), 88.1 (Cq), 90.3 (CH_{furan}), 110.5, 124.7 and 126.6 ($5CH_{Ar}$), 127.2 (Cq), 128.7 and 129.8 ($2CH_{Ar}$), 129.9, 130.1 and 130.2 (3Cq), 139.6 (CH_{Ar}), 150.5 (Cq), 157.1, 162.6 and 176.0 ($3CO_{amide}$), 188.7 (CO_{ketone}); MS, m/z: 455 ($M^{+\bullet}$).

ACKNOWLEDGEMENT

The authors would like to thank the Research Council of Mazandaran University for financial support.

CONFLICT OF INTEREST

There are no conflicts to declare.

ORCID

Robabeh Baharfar https://orcid.org/0000-0002-8215-1851
Daryoush Zareyee https://orcid.org/0000-0001-9405-5683

REFERENCES

[1] P. Saraswat, G. Jeyabalan, M. Z. Hassan, M. U. Rahman, N. K. Nyola, *Synth. Commun.* **2016**, *46*(20), 1643.

[2] P. X. Jiang, Y. Sun, J. Yao, Y. Cao, M. Kai, N. He, X. Zhang, Y. Wang, R. Wang, *Adv. Synth. Catal.* **2012**, *354*, 917.

[3] G. Bhaskar, Y. Arun, C. Balachandran, C. Saikumar, P. T. Perumal, *Eur. J. Med. Chem.* **2012**, *51*, 79.

[4] M. M. Santos, *Tetrahedron* **2014**, *70*(52), 9735.

[5] D. Cheng, Y. Ishihara, B. Tan, C. F. Barbas III, *ACS Catal.* **2014**, *4*(3), 743.

[6] H. A. Burch, R. E. White, G. C. Wright, M. M. Goldenberg, *J. Pharm. Sci.* **1980**, *69*(1), 107.

[7] S. Ahadi, H. R. Khavasi, A. Bazgir, *Chem. Eur. J.* **2013**, *19*, 12 553.

[8] R. Baharfar, S. Asghari, F. Zaheri, N. Shariati, *C. R. Chim.* **2017**, *20*(4), 359.

[9] D. Zhang, S. Johnson, H. L. Cui, F. Tanaka, *Asian J. Chem.* **2014**, *3*(4), 391.

[10] J. Xu, J. Cao, C. Fang, T. Lu, D. Du, *Org. Chem. Front.* **2017**, *4*(4), 560.

[11] Y. Zhang, Y. Lu, W. Tang, T. Lu, D. Du, *Org. Biomol. Chem.* **2014**, *12*(19), 3009.

[12] Y. L. Liu, X. Wang, Y. L. Zhao, F. Zhu, W. P. Zeng, L. Chen, C. H. Wang, X. L. Zhao, J. Zhou, *Angew. Chem. Int. Ed.* **2013**, *52*, 13 980.

[13] L. H. Sun, L. T. Shen, S. Ye, *Chem. Commun.* **2011**, *47*, 10 136.

[14] G. Bergonzini, P. Melchiorre, *Angew. Chem. Int. Ed.* **2012**, *124*(4), 995.

[15] H. Veisi, A. Sedrpoushan, B. Maleki, M. Hekmati, M. Heidari, S. Hemmati, *Appl. Organomet. Chem.* **2015**, *29*(12), 834.

[16] B. Maleki, S. Babaee, R. Tayebee, *Appl. Organomet. Chem.* **2015**, *29*(6), 408.

[17] E. Eidi, M. Z. Kassaee, Z. Nasresfahani, P. T. Cummings, *Appl. Organomet. Chem.* **2018**, *32*, 4573.

[18] M. Tajbakhsh, M. Farhang, R. Hosseinzadeh, Y. Sarrafi, *RSC Adv.* **2014**, *4*, 23 116.

[19] M. Tajbakhsh, H. Alinezhad, M. Nasrollahzadeh, T. A. Kamali, *J. Colloid Interface Sci.* **2016**, *471*, 37.

[20] P. Van Der Voort, D. Esquivel, E. De Canck, F. Goethals, I. Van Driessche, F. J. Romero-Salguero, *Chem. Soc. Rev.* **2013**, *42*, 3913.

[21] B. Karimi, F. B. Rostami, M. Khorasani, D. Elhamifar, H. Vali, *Tetrahedron* **2014**, *70*, 6114.

[22] B. Karimi, D. Elhamifar, O. Yari, M. Khorasani, H. Vali, J. H. Clark, A. J. Hunt, *Chem. Eur. J.* **2012**, *18*, 13 520.

[23] B. Karimi, D. Elhamifar, J. H. Clark, A. Hunt, *Chem. Eur. J.* **2010**, *16*, 8047.

[24] B. Karimi, D. Elhamifar, J. H. Clark, A. Hunt, *J. Org. Biomol. Chem.* **2011**, *9*, 7420.

[25] D. Elhamifar, B. Karimi, J. Rastegar, M. H. Banakar, *Chem. Cat. Chem.* **2013**, *5*, 2418.

[26] B. Karimi, A. Maleki, D. Elhamifar, J. H. Clark, A. Hunt, *Chem. Commun.* **2010**, *46*, 6947.

[27] M. Nasr-Esfahani, D. Elhamifar, T. Amadeh, B. Karimi, *RSC Adv.* **2015**, *5*, 13 087.

[28] D. Elhamifar, F. Hosseinpoor, B. Karimi, S. Hajati, *Microporous Mesoporous Mater.* **2015**, *204*, 269.

[29] B. Karimi, M. Khorasani, F. Bakhshandeh Rostami, D. Elhamifar, H. Vali, *ChemPlusChem* **2015**, *80*, 990.

[30] M. Gholinejad, B. Karimi, A. Aminianfar, M. Khorasani, *ChemPlusChem* **2015**, *80*(10), 1573.

[31] D. Elhamifar, S. Kazempoor, B. Karimi, *Catal. Sci. Technol.* **2016**, *6*(12), 4318.

[32] J. F. Liu, G. B. Jiang, Y. G. Chi, Y. Q. Cai, Q. X. Zhou, J. T. Hu, *Anal. Chem.* **2003**, *75*, 5870.

[33] J. F. Liu, Y. G. Chi, G. B. Jiang, C. Tai, J. F. Peng, J. T. Hu, *J. Chromatogr. A* **2004**, *1026*, 143.

[34] D. W. Armstrong, L. He, Y. S. Liu, *Anal. Chem.* **1999**, *71*, 3873.

[35] J. L. Anderson, D. W. Armstrong, *Anal. Chem.* **2003**, *75*, 4851.

[36] J. Ding, T. Welton, D. W. Armstrong, *Anal. Chem.* **2004**, *76*, 6819.

[37] R. Baharfar, N. Shariati, *C. R. Chim.* **2014**, *17*(5), 413.

[38] N. Porahmad, R. Baharfar, *Res. Chem. Intermed.* **2018**, *44*(1), 305.

[39] R. Baharfar, R. Azimi, *Synth. Commun.* **2014**, *44*(1), 89.

[40] R. Baharfar, S. Mohajer, *Catal. Lett.* **2016**, *146*(9), 1729.

[41] C. Li, J. Yang, X. Shi, J. Liu, Q. Yang, *Microporous Mesoporous Mater.* **2007**, *98*, 220.

[42] M. M. Abolghasemi, B. Karimi, V. Yousefi, *Anal. Chim. Acta* **2013**, *804*, 280.

[43] M. Kruk, M. Jaroniec, *Chem. Mater.* **2001**, *13*, 3169.

SUPPORTING INFORMATION

Additional supporting information may be found online in the Supporting Information section at the end of the article.

How to cite this article: Baharfar R, Zareyee D, Allahgholipour SL. Synthesis and characterization of MgO nanoparticles supported on ionic liquid-based periodic mesoporous organosilica (MgO@PMO-IL) as a highly efficient and reusable nanocatalyst for the synthesis of novel spirooxindole-furan derivatives. *Appl Organometal Chem*. 2019;e4805. https://doi.org/10.1002/aoc.4805